



**HAL**  
open science

## Charge Migration Manifests as Attosecond Solitons in Conjugated Organic Molecules

Francois Mauger, Aderonke S Folorunso, Kyle A Hamer, Cristel Chandre,  
Mette B Gaarde, Kenneth Lopata, Kenneth J Schafer

► **To cite this version:**

Francois Mauger, Aderonke S Folorunso, Kyle A Hamer, Cristel Chandre, Mette B Gaarde, et al..  
Charge Migration Manifests as Attosecond Solitons in Conjugated Organic Molecules. 2021. hal-  
02866922v2

**HAL Id: hal-02866922**

**<https://hal.science/hal-02866922v2>**

Preprint submitted on 16 Dec 2021 (v2), last revised 13 Jan 2022 (v3)

**HAL** is a multi-disciplinary open access archive for the deposit and dissemination of scientific research documents, whether they are published or not. The documents may come from teaching and research institutions in France or abroad, or from public or private research centers.

L'archive ouverte pluridisciplinaire **HAL**, est destinée au dépôt et à la diffusion de documents scientifiques de niveau recherche, publiés ou non, émanant des établissements d'enseignement et de recherche français ou étrangers, des laboratoires publics ou privés.

# Charge Migration Manifests as Attosecond Solitons in Conjugated Organic Molecules

François Mauger,<sup>\*,†</sup> Aderonke S. Folorunso,<sup>‡</sup> Kyle A. Hamer,<sup>†</sup> Cristel Chandre,<sup>¶</sup>  
Mette B. Gaarde,<sup>†</sup> Kenneth Lopata,<sup>‡,§</sup> and Kenneth J. Schafer<sup>†</sup>

<sup>†</sup>*Department of Physics and Astronomy, Louisiana State University, Baton Rouge,  
Louisiana 70803, USA*

<sup>‡</sup>*Department of Chemistry, Louisiana State University, Baton Rouge, Louisiana 70803,  
USA*

<sup>¶</sup>*CNRS, Aix Marseille Univ, Centrale Marseille, I2M, Marseille, France*

<sup>§</sup>*Center for Computation and Technology, Louisiana State University, Baton Rouge,  
Louisiana 70803, USA*

E-mail: fmauger@lsu.edu

## Abstract

We report theoretical investigations of charge migration that takes place along the backbone of conjugated hydrocarbons, simulated using time-dependent density functional theory and analyze using tools from nonlinear dynamics. In this electron-density framework charge migration modes emerge as attosecond solitons and the same type of solitary-wave dynamics manifests in full molecular simulations and in a simplified model of the conjugated  $\pi$  system. These attosecond-soliton modes result from a balance between dispersion and nonlinear effects tied to time-dependent multi-electron interactions. The soliton-mode mechanism, and the nonlinear tools we use to analyze it, pave the way for understanding migration dynamics in a broad range of organic

molecules. For instance, we demonstrate the opportunities for chemically steering charge migration via molecular functionalization, which can alter both the initially localized electron perturbation and its subsequent time evolution.

The movement of electrons and holes in matter regulates many physical and chemical processes such as chemical reactions, photosynthesis and photovoltaics, and charge transfer.<sup>1,2</sup> These dynamics can reach down to the Angstrom and attosecond spatio-temporal scales, and are commonly referred to as charge migration (CM).<sup>3-8</sup> At the fastest time scales, CM is understood as the purely electronic-driven dynamics that takes place before nuclei have time to move. It can be the precursor for many of the down-stream processes mentioned above,<sup>2,9-11</sup> and therefore a means of understanding and ultimately steering them via charge-directed reactivity.<sup>12,13</sup>

The study of molecular CM is a formidable endeavor. Experimental studies require coherent probes with attosecond resolution,<sup>2,6,14</sup> as enabled by the continuous progress in x-ray and table-top high harmonic sources over the past few decades.<sup>1</sup> Theoretical investigations of CM necessitate models with multiple interacting electrons,<sup>15,16</sup> even when nuclear motion is ignored.<sup>17-21</sup> Furthermore, systematic studies of the mechanisms responsible for regulating CM involve the analysis of systems with a large number of coupled degrees of freedom.

In this work, we show that periodic modes of CM with a localized hole that travels back and forth along the molecule's conjugated chain emerge as attosecond solitons. These solitary waves represent a balance between dispersion and nonlinear effects that are driven by time-dependent multi-electron interactions. The attosecond-soliton picture provides a generic mechanism for sustained CM in organic molecules that does not rely on nonphysical molecular orbitals for its description. Notably, we find that the same molecule can support several of these CM modes with periods varying by several hundred attoseconds. We discuss the implication of our results for future theoretical and experimental CM studies, including the opportunities for chemically steering CM by molecular functionalization.

Recent simulations demonstrated that halohydrocarbons support facile CM, via hopping

between  $\pi$  bonds.<sup>21</sup> The result was obtained for a hole initially localized on the halogen, meaning that the robustness of the CM with respect to changes in the initial hole remains unexplored. Here we address this question using bromohexatriyne for illustration. Specifically, we investigate the influence of the initial hole localization on the CM it induces. We compute CM dynamics in the singly ionized cation with *ab initio* time-dependent density-functional theory (TDDFT) in NWChem,<sup>22,23</sup> using cc-pVDZ and Stuttgart RLC-ECP Gaussian basis sets together with the PBE0 exchange-correlation functional (see SI for complete simulation details).

Figure 1 shows the result of a CM-period analysis in bromohexatriyne. The more the initial hole is localized the further away its electronic structure is from the ground-state distribution. This translates into a higher level of molecular excitation, which we indicate along the lower x axis. We vary the portion of the electron hole initially localized on the Br atom, as discussed in the Computational details below, and follow its subsequent time evolution. We then compute the frequency of CM modes that move the density between the Br and final C $\equiv$ C–H groups in the target – orange markers in figure 1. The period of the CM increases with the initial-hole localization (excitation energy). This increase happens in a step-wise fashion over ranges of initial conditions that lead to essentially the same CM period. Note the two distinctive plateaus between 1.7 eV and 3.3 eV, and 4.3 eV and 6 eV, highlighted with the dashed grey lines in the figure. In each of those plateaus, CM motions corresponds to the hole periodically propagating back and forth through the entire chain by hopping between the Br and adjacent pairs of C $\equiv$ C – see reference (<sup>21</sup>) for sample CM motions.

The CM-modes associated with each of the plateaus in figure 1 correspond to regions of the parameter space over which different initial conditions lead to the same CM motion, all with essentially the same period. In other words, the overall CM dynamics is not so much determined by the details of the individual electronic degrees of freedom, nor the competition between them, than it is driven by their collective response. This type of collective behavior is

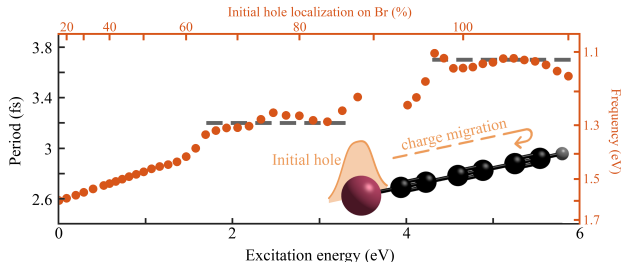


Figure 1: Main frequency of the bromohexatriyne CM motion that moves the hole throughout the entire molecule, between the Br and final  $\text{C}\equiv\text{C}-\text{H}$  groups, when varying the degree of localization of the initial hole on the Br. The left/bottom axes show the corresponding CM period and excitation energy, respectively.

usually referred to as synchronization and has been identified throughout physics, engineering and biology.<sup>24–26</sup> Below we explain how this synchronization emerges through a solitary-wave mechanism, providing a novel way to understand CM dynamics in real space directly in time domain. Notably, the type of parametric stability exhibited in the plateaus is essential for experimental applications as it provides a robustness of the migration dynamics against uncertainties in the way the hole is created.

To facilitate further the nonlinear analysis of CM modes, we build a one-dimensional model of the  $\pi$  system of alkene/alkyne hydrocarbons for which we can perform extensive computations and detailed analyses (see SI). We first focus on the conjugated carbon chain alone and discuss the effect of functionalization at the end of the paper. Figure 2 shows the results of a CM-period analysis akin to that of bromohexatriyne above. For each initial hole configuration we compute the field-free CM dynamics and extract the main frequency component of any motion that moves the hole density between the two ends of the molecule (dark orange markers). The results are strikingly similar to the 3D bromohexatriyne case. First, the period of the CM increases with increasing molecular excitation energy: initially more localized holes lead to slower CM. Second, this increase proceeds in an almost step-wise fashion via a series of plateaus. Within each of these plateaus, the period of the CM is essentially independent of the excitation energy or, equivalently, of the details of how the hole was initialized.

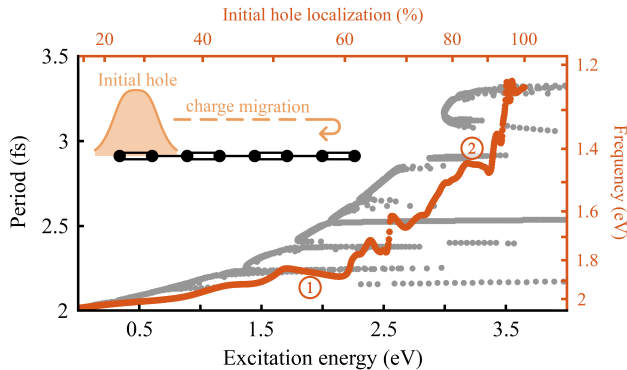


Figure 2: (dark orange markers) Similar CM-frequency/period analysis as in figure 1 for a model conjugated  $\pi$  system with four carbon dimers – see inset. For comparison, light grey dots show a direct computations of periodic CM modes in the full phase space of the model  $\pi$  system.

In figure 3 (a,b) we show the temporal evolution of sample densities associated with two different plateaus of figure 2, labeled 1 and 2 on the figure. In our model  $\pi$  system, these dynamics are best understood by looking at the density contribution from the Kohn-Sham (KS) orbital in which we introduce the initial hole. Both panels reveal qualitatively similar motions where the initial electron density, instead of spreading, remains localized in space and periodically propagates through the entire  $\pi$  system like a particle. We observe qualitatively similar results in the other plateaus of figure 2. Notably, when looking at the CM dynamics in terms of the physical quantity, the hole density, we see that it follows the same type of back-and-forth motion as the unpaired KS electron density – compare panels (b) and (c). We understand the correspondence between the two as the result of the orthonormality of the KS orbitals in TDDFT (see the Computational details below): The localized density of panel (b) corresponds to an unpaired KS-orbital channel, which therefore contributes a single electron to the total one-body density. The other KS orbitals, which are forced to “stay away” from it via orthogonality conditions, all correspond to fully filled KS channels and therefore contribute two electrons to the density ultimately leading to the matching hole density in panel (c).

To better understand the mechanism that regulates the particle-like hole dynamics shown in figure 3, we formally decompose the TDDFT Hamiltonian operator  $\hat{\mathcal{H}}_{\text{eff}}$  (see Computa-

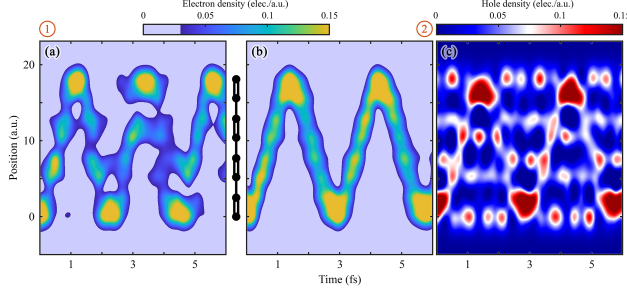


Figure 3: (a,b) Electron density contribution from the unpaired KS-orbital channel in which we introduce the initial localized-hole perturbation – see text. (c) Hole density associated with panel (b). The overhead labels ① and ② indicate the plateaus of figure 2 from which these are taken.

tional details) into its linear and nonlinear parts  $\hat{\mathcal{H}}_{\text{eff}}[\rho(t)] = \hat{\mathcal{H}}_{\text{eff}}[\rho_{\text{GS}}] + \Delta\hat{\mathcal{H}}_{\text{eff}}[\rho(t)]$ , where  $\rho_{\text{GS}}$  is the ground-state one-body density of the molecular cation. Modeling the CM as a beating of molecular orbitals (MO) amounts to neglecting the nonlinear part  $\Delta\hat{\mathcal{H}}_{\text{eff}}[\rho(t)]$ . We find that the linearized MO-beating approximation yields qualitatively different results from those of figure 2 and we understand the inadequacy of the MO-beating picture as follows (also illustrated in the SI): MOs are delocalized over the entire  $\pi$  system and thus, in order to obtain a tightly localized electron density over a portion of the chain, one needs a coherent superposition of multiple MO wave functions. Then, the mismatch in the energy spacing between these MOs would lead to a decoherence, and thus spread, of the electronic density, which we do not observe here. This shows that the dispersion associated with the linear part of  $\hat{\mathcal{H}}_{\text{eff}}[\rho(t)]$  is cancelled by nonlinear effects associated with the nonlinear component  $\Delta\hat{\mathcal{H}}_{\text{eff}}[\rho(t)]$ , ultimately leading to the non-dispersing solitary-wave dynamics shown in figure 3.

To conclude our nonlinear analysis, we return to figure 2 and note that the CM-period analysis starting from a hole on one end of the system (dark orange markers) explores only a narrow portion of the total phase space for CM dynamics. One could design different ways to generate the initial hole, each potentially exploring a different portion of the phase space. To more fully explore the phase space in our model system, we carry out a direct systematic search for periodic CM modes that exhibit a traveling solitary wave similar to figure 3 (b,c),

in the full parameter space of the model  $\pi$  system. We show the period and excitation-energy of these CM modes with light grey markers in figure 2. As a whole, these results give a very clear picture of how the dynamics of particle-like CM is organized in the phase space of the  $\pi$  system: The “ladder” of extended plateaus again shows that essentially the same CM period can be observed over a wide range of excitation energy, often spanning more than one eV. We also recover the general trend that slower CM modes are only available for more excited electronic configurations of the target – note the lack of periodic CM modes in the upper-left corner of the figure.

In figure 2, the comparison between the periodic CM modes and previous CM-period analysis is stunning – light grey and dark orange markers, respectively: All the plateaus in the latter match a set of periodic modes in the former. In other words, these periodic CM modes form the dynamical skeleton that regulates the CM we observed when creating an *ad hoc* localized hole at one end of the  $\pi$  system. The “cleanliness” of that motion – *e.g.*, figure 3 (a) *vs* (b) – depends on how close the initial condition puts the electronic configuration to a suitable periodic CM mode it can mimic. Altogether this suggests a two-pronged approach to CM studies: (i) asking whether the molecule of interest supports periodic soliton CM modes. If so, then (ii) tailor the ionization process to create an initial hole that results in these CM mode(s) of interest.

In conclusion, we have performed detailed analyses of CM in conjugated organic molecules using tools from nonlinear dynamics. In the density picture we showed that periodic CM modes, with a hole traveling back-and-forth through the  $\pi$  system in a particle-like manner, emerge as solitary waves. This mechanism is fundamentally different from the few-orbital beating pictures that have previously been employed<sup>6,9,17</sup> and is driven by time-dependent multi-electron interactions. Similar solitary-wave CM modes are observed in both full-dimensional simulations and simplified conjugated model. Our results suggests that the particle-like CM motions we identify emerge as a result of the dynamical mean-field interaction alone. Long-range many-electron interactions are a hallmark of conjugated organic

molecules, which makes the possibility for sustained CM motions widely available in these systems. Surprisingly, our analysis reveals that the same molecule can support several soliton CM modes with very different periods. In the full bromohexatriyne simulations of figure 1, the two CM modes are 500 as apart. For the model  $\pi$  system shown in figure 2, the identified CM periods vary over a range of about 1 fs.

Finally, practical application of the principles we report requires creating a localized hole in one region of the molecule. Experiments and simulations have shown that strong-field ionization of halohydrocarbons can result in a local hole on the halogen.<sup>7,27,28</sup> To determine the relationship between functionalization and attosecond soliton CM modes, in the model  $\pi$  system, we emulate halogen functionalization by adding an atomic center at one end of the conjugated-carbon chain. When varying the properties of this atomic center we have found that it can change, or even altogether disable, CM observed in the rest of the chain (see SI figure S1 for an illustration). This speaks to the idea of chemical control of CM, where a functional group added to a conjugated organic system can act as a bias and alter the ability of the rest of the molecule to support periodic CM modes. More broadly, the possibility for altering a molecule’s ability to support CM through changes in its electronic configuration opens the door to doing the same thing through external knobs like laser fields: The laser would selectively switch sustained CM “on” or “off” in the target sample by enabling or preventing its CM modes.

## Computational details

In all simulations we use TDDFT, in the Kohn-Sham (KS) formalism,<sup>29</sup> with fixed nuclei

$$i\partial_t\phi_k(\vec{r}; t) = \hat{\mathcal{H}}_{\text{eff}}[\rho](\vec{r})\phi_k(\vec{r}; t). \quad (1)$$

In the molecular cation with  $N - 1$  active electrons, the one-body density reads

$$\rho(\vec{r}; t) = \sum_{k=1}^{N-1} |\phi_k(\vec{r}; t)|^2. \quad (2)$$

Following Pauli’s exclusion principle, the KS orbitals  $\{\phi_k\}_k$  are orthonormal wave function in their spin and space coordinates. The one-body density provides a real-space representation of the electronic-charge distribution in the molecule. From it, the hole density  $\rho_h(\vec{r}; t) = \rho_N(\vec{r}) - \rho(\vec{r}; t)$  is computed by taking the difference with the neutral’s ground-state density  $\rho_N(\vec{r})$ .

In this work, we investigate the influence of the initial hole localization on its subsequent CM dynamics. Specifically, we systematically and continuously vary the initial degree of localization of a one-electron hole around one end of the conjugated system. By convention 0% localization corresponds to the cation ground state and 100% to a fully localized hole. To build the initial hole for the Gaussian basis-set TDDFT simulations, we use constrained DFT (cDFT),<sup>30</sup> which combines standard energy minimization techniques with the constraint of having a certain amount of the hole localized around a specific center in the molecule. This approach allows us to consistently impose the initial-hole configuration without involving *ad hoc* MO mixing. The cDFT approach was shown to be successful in a previous study of CM in halocarbons.<sup>21</sup> For the model  $\pi$  system, we build our variably-localized hole configuration with a linear combination of a few occupied and unoccupied MOs of the corresponding cation. Following the initialization of the hole, we compute the subsequent TDDFT dynamics in the full, unrestricted TDDFT framework of equations (1,2), for both the real molecule and model system.

## Acknowledgement

We thank L.F. DiMauro and R.R. Jones for helpful discussions on this work. This work was supported by the U.S. Department of Energy, Office of Science, Office of Basic Energy

# Supporting Information: Charge Migration Manifests as Attosecond Solitons in Conjugated Organic Molecules

## TDDFT simulations

For full-dimensional ab-initio TDDFT simulations in bromohexatriyne,<sup>21</sup> we use an all-electron, spin polarized level of theory with the hybrid PBE0 functional, cc-pVDZ basis set for the H and C atoms and Stuttgart RLC ECP for Br, as implemented in the NWChem package.<sup>22,23</sup> Following the initial hole configuration (see below), we time propagate the TDDFT dynamics for 29 fs (1200 a.u.) with a time step of 0.2 a.u. (4.8 as).

For the reduced  $\pi$ -system model (see next section), we use spin-restricted TDDFT with local-density approximation (LDA) Slater-exchange and correlation potentials<sup>31</sup> and an average-density self-interaction correction (ADSIC).<sup>32</sup> For the time propagation, we use a second-order Strang splitting for a total duration of 30 fs with a time step of 0.05 a.u. (1.2 a.s.).

## Reduced $\pi$ -system model

We systematically build our reduced  $\pi$  system from one-dimensional (1D) carbon chains, denoted  $(C_2)_n$ , with  $n$  the number of pairs of “C” centers. These chains are the 1D analog to 3D alkenes, without the hydrogen centers. We use soft-Coulomb<sup>33</sup> effective potentials to describe electron interactions, parameterized as  $V_{sc}[Z, a](x) = -\frac{Z}{\sqrt{x^2+a^2}}$ , with  $Z$  the effective charge and  $a$  the softening parameter. For electron-electron interactions we take a softening parameter  $a_{ee} = \sqrt{2}$ . In the model  $\pi$  system, each C center contributes one electron with  $Z_C = 1$ . We set the respective positions for the atomic centers to emulate conjugation-like bonding by using slightly different inter-atomic distances within and between  $C_2$  pairs,

respectively set to 2.5 a.u. and 2.7 a.u. We chose these distances to be comparable to the ones from full-dimensional (functionalized) alkenes. Finally, we select the softening parameter  $a_C = 1$  for which we consistently find reasonable electronic properties throughout the  $(C_2)_n$  family, both in terms of molecular orbital energies and shapes.

For brevity, we mainly show results for the  $(C_2)_4$  system. We systematically find similar results – multiple plateaus in the CM-period analysis associated with periodic CM modes with a traveling particle-like hole, longer CM periods accessible only to more excited configurations, etc. – for the other members of the  $(C_2)_n$  family.

To functionalize the model  $\pi$  system we add a single atomic “X” center with  $Z_X = 2$  at one end of the molecule, meant to emulate a halogen group. We then use the softening parameter  $a_X$  and distance between the function and chain to tune the coupling/hybridization between the two.

Figure 4 illustrates how functionalization could be used to control CM dynamics. Here we functionalize the model  $\pi$  system by adding a single atomic center at one of its ends, meant to emulate a halogen function. We start the variably-localized hole on the chain side of the compound and compare the CM dynamics for two different functionalization configurations, here controlled with the distance between the function-atom and chain. Panel (a) compares the result of a CM-period analysis for two functionalized  $\pi$  system configuration. The two analyses show qualitatively different results: The configuration with  $R_{XC}=3$  reproduces the successions of plateaus with longer periods as the excitation energy increases of the chain alone – compare to figure 2 of the main document. On the other hand, the configuration with  $R_{XC}=4$  lacks the plateau structure. This suggests that only the former configuration supports sustained solitary-wave CM modes, as illustrated in the sample CM motions of panels (b,c).

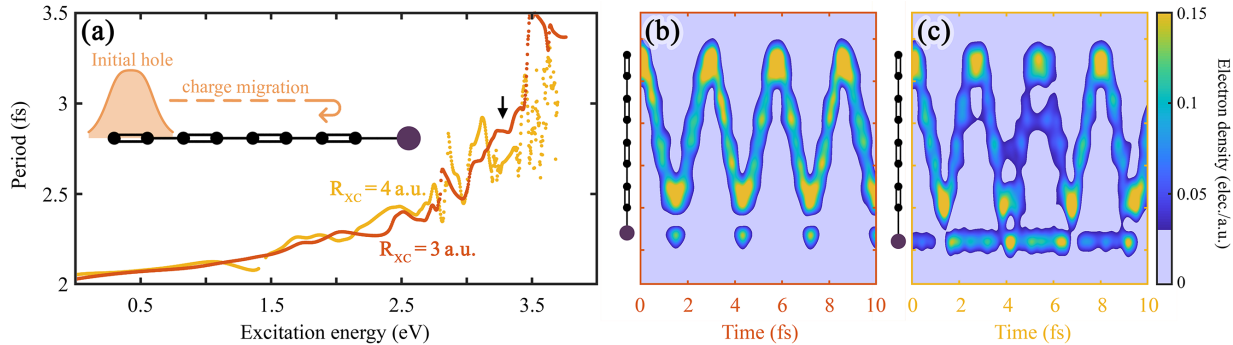


Figure 4: (a) Similar to figures 1 and 2 of the main document: CM-period analysis for two functionalized model  $\pi$  systems, where we initially set the variably localized hole on the chain side of the molecule. Here we model two different chemical functionalizations by varying the distance between the function-atom and the chain – 4 and 3 a.u., as labeled next to the curves. (b,c) sample CM motions for each model with initial conditions labeled by the arrow in panel (a).

## Variable initial hole configuration

We initialize all simulations with a one-electron hole in the conjugated system of the molecular cation.

For the model  $\pi$  system, we take an intuitive approach to building the initial condition using a single parameter to control the initial hole localization. In this system, the molecular cation has one unpaired KS orbital, while the other ones are fully filled. In the unpaired KS-orbital channel, we linearly mix a one-electron wave function localized around an end C dimer with the delocalized cation’s ground state highest-occupied molecular orbital; the initial localization of the hole is controlled by this mixing coefficient. We then reorthonormalize the remaining paired KS orbitals. In the end, the difference in the number of electrons contributed by the unpaired and paired KS orbital yields the relative deficit of electronic density over one of the final C dimers – see figure 5.

For 3D TDDFT simulations of bromohexatriyne, the use of the cDFT method was described in reference.<sup>21</sup> In reference<sup>21</sup> all CM simulations were initialized with the constraint of having exactly one electron hole on the halogen center. Here, instead, we keep the overall one-electron hole but vary the amount of that hole that is constrained to be localized around the Br center – see figure 6.

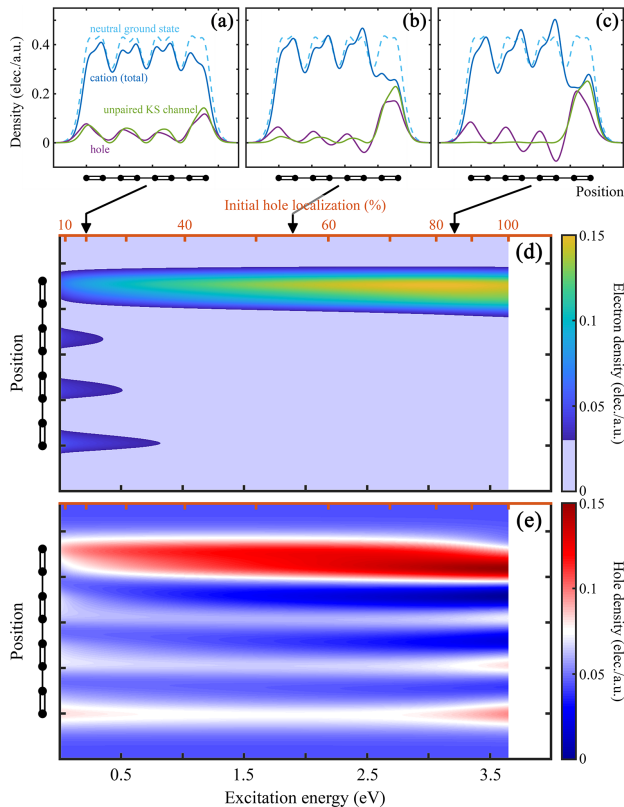


Figure 5: Variation of the initial electron/hole configuration we use for the CM-period analysis of the model  $\pi$  system. (a-c) Samples of the initial electron and hole density distributions along the molecular backbone for 20%, 55%, and 85% localization, respectively. (d) Initial electron density in the unpaired Kohn-Sham (KS) orbital we use as initial condition in the CM-period analysis of figure 2. (e) Initial hole density associated with (d). Note that panels (d,e) use the same colormaps as in figure 3. The colormaps stop at 100% initial hole localization because our initial-condition mixing scheme has an upper bound for the excitation energy it can induce in the cation. On the other hand, we do not have the same upper limit when directly searching for periodic CM modes in the full parameter space, and we can therefore achieve the higher excitation energies shown in figure 2.

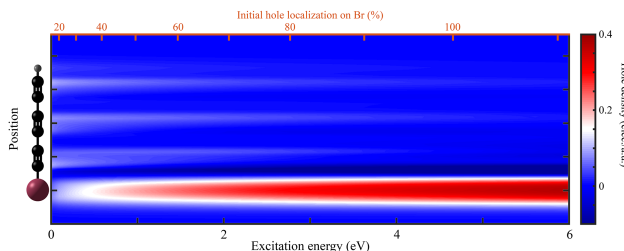


Figure 6: Like in figure 5 (e), variation of the initial hole configuration for the CM-period analysis of bromohexatriyne of figure 1. Here the constrained DFT (cDFT) algorithm enables us to impose over 100% initial localization of the hole on the Br end.

## CM-period analysis

Generally speaking, we track the variation of the main frequency component, or equivalently the period, of the CM motion as a function of a continuously-varied initial hole configuration.<sup>34,35</sup> While we use slightly different implementation of the CM-period for the analysis of the full 3D TDDFT simulations and the model  $\pi$  system, the underlying idea is the same in both cases: To analyze CM motions across the entire molecule, we construct a complex-valued scalar signal  $s_{\text{FMA}}(t) = s_l(t) + i s_r(t)$  by computing the amount of electron/hole density around the left and right ends of the molecule, respectively  $s_{l,r}$ . For the CM-period analysis itself, we use the time interval  $10 \text{ fs} \leq t \leq 30 \text{ fs}$ : We discard the first 10 fs to avoid transient effects associated with the sudden introduction of the localized perturbation in the system. We have checked that including them in the analysis has only cosmetic effects and does not change our results and conclusions.

For the 3D TDDFT simulations of bromohexatriyne (figure 1 in the main document), we compute  $s_{l,r}$  by simply integrating the hole density around the Br (left side of the median plane to the Br-C bond) and around the  $-\text{C}\equiv\text{C}-\text{H}$  (right side of the median plane to the final  $\equiv\text{C}-\text{C}\equiv$  bond) groups, respectively.

For the model  $\pi$  system (figure 2 in the main document), we compute  $s_{l,r}$  by projecting the electron density contribution for the unpaired KS orbital over the end  $\text{C}_2$  dimers. We choose this projection for consistency with the results of figure 3 (a,b) where we showed that the underlying organization of the CM dynamics is best apparent in this KS-orbital channel. We have checked that we obtain essentially the same results when projecting the entire hole density on the same end dimers.

Figure 7 compares the full TDDFT dynamics, including *time-dependent* electron-electron interactions, with its linearized approximation  $\Delta\hat{\mathcal{H}}_{\text{eff}} = 0$  (see main document), which reduces the dynamics to the beating between molecular orbitals. Because of the lack of synchronization/CM soliton in the linearized approximation, we do not observe sustained periodic CM modes and instead obtain multiple leading frequency components in the analysis

discussed above.

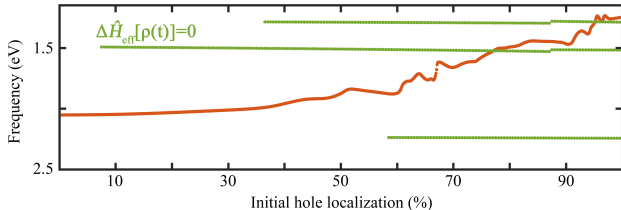


Figure 7: Comparison of the CM-frequency (period) analysis for the full TDDFT dynamics with its linearized approximation of  $\Delta\hat{\mathcal{H}}_{\text{eff}} = 0$  (see main document), which reduces the dynamics to the beating between molecular orbitals. The orange curve is identical to the CM-period analysis of figure 2. The green horizontal lines show the frequency components using the same initial conditions but with the nonlinear component  $\Delta\hat{\mathcal{H}}_{\text{eff}}$  ignored in the time propagation. Note the inverted frequency  $y$  axis to match other CM-period analyses

## Periodic CM mode search

The TDDFT system of equations (1,2) in the main document has an infinite number of degrees of freedom, which makes it impractical for a direct computation of periodic CM modes. Instead, we employ a two-step approach: First, we restrict the dynamics to few occupied and unoccupied MOs of the corresponding cation and use a nonlinear solver – here the Levenberg-Marquardt Method as implemented in MATLAB<sup>®</sup> – to find periodic motions in that restricted space. Then, we use those restricted periodic modes as initial conditions in unrestricted TDDFT simulations and check that they still correspond to periodic motions. We stress that, with this approach, the restricted computations only serve as an intermediary to determining periodic CM modes in the same TDDFT framework we use for our other CM simulations.

## References

- (1) Krausz, F.; Ivanov, M. Attosecond physics. *Rev. Mod. Phys.* **2009**, *81*, 163–234.
- (2) Calegari, F.; Trabattoni, A.; Palacios, A.; Ayuso, D.; Castrovilli, M. C.; Green-

- wood, J. B.; Decleva, P.; Martín, F.; Nisoli, M. Charge migration induced by attosecond pulses in bio-relevant molecules. *J. Phys. B: At. Mol. Opt. Phys.* **2016**, *49*, 142001.
- (3) Breidbach, J.; Cederbaum, L. S. Universal Attosecond Response to the Removal of an Electron. *Phys. Rev. Lett.* **2005**, *94*, 033901.
- (4) Lünemann, S.; Kuleff, A. I.; Cederbaum, L. S. Ultrafast charge migration in 2-phenylethyl-N,N-dimethylamine. *Chem. Phys. Lett.* **2008**, *450*, 232–235.
- (5) Smirnova, O.; Mairesse, Y.; Patchkovskii, S.; Dudovich, N.; Villeneuve, D.; Corkum, P.; Ivanov, M. Y. High harmonic interferometry of multi-electron dynamics in molecules. *Nature* **2009**, *460*, 1476–1487.
- (6) Calegari, F.; Ayuso, D.; Trabattoni, A.; Belshaw, L.; De Camillis, S.; Anumula, S.; Frassetto, F.; Poletto, L.; Palacios, A.; Decleva, P.; Greenwood, J.; Martín, F.; Nisoli, M. Ultrafast electron dynamics in phenylalanine initiated by attosecond pulses. *Science* **2014**, *346*, 336–339.
- (7) Kraus, P.; Mignolet, B.; Baykusheva, D.; Rupenyan, A.; Horný, L.; Penka, E.; Grassi, G.; Tolstikhin, O.; Schneider, J.; Jensen, F.; Madsen, L.; Bandrauk, A.; Remacle, F.; Wörner, H. Measurement and laser control of attosecond charge migration in ionized iodoacetylene. *Science* **2015**, *350*, 790–795.
- (8) Kuleff, A. I.; Kryzhevoi, N. V.; Pernpointner, M.; Cederbaum, L. S. Core Ionization Initiates Subfemtosecond Charge Migration in the Valence Shell of Molecules. *Phys. Rev. Lett.* **2016**, *117*, 093002.
- (9) Remacle, F.; Levine, R. D. An electronic time scale in chemistry. *Proceedings of the National Academy of Sciences* **2006**, *103*, 6793–6798.
- (10) Lépine, F.; Ivanov, M. Y.; Vrakking, M. J. J. Attosecond molecular dynamics: fact or fiction? *Nat. Photon.* **2014**, *8*, 1749–1753.

- (11) Despré, V.; Marciniak, A.; Loriot, V.; Galbraith, M. C. E.; Rouzée, A.; Vrakking, M. J. J.; Lépine, F.; Kuleff, A. I. Attosecond Hole Migration in Benzene Molecules Surviving Nuclear Motion. *J. Chem. Phys. Lett.* **2015**, *6*, 426–431.
- (12) Weinkauff, R.; Schlag, E. W.; Martinez, T. J.; Levine, R. D. Nonstationary Electronic States and Site-Selective Reactivity. *J. Phys. Chem. A* **1997**, *101*.
- (13) Remacle, F.; Levine, R.; Ratner, M. Charge directed reactivity: a simple electronic model, exhibiting site selectivity, for the dissociation of ions. *Chem. Phys. Lett.* **1998**, *285*, 25–33.
- (14) Tuthill, D. R.; Mauger, F.; Scarborough, T. D.; Jones, R. R.; Gaarde, M. B.; Lopata, K.; Schafer, K. J.; DiMauro, L. F. Multidimensional molecular high-harmonic spectroscopy: A road map for charge migration studies. *J. Mol. Spectro.* **2020**, *372*, 111353.
- (15) Vacher, M.; Bearpark, M. J.; Robb, M. A.; Malhado, J. P. Electron Dynamics upon Ionization of Polyatomic Molecules: Coupling to Quantum Nuclear Motion and Decoherence. *Phys. Rev. Lett.* **2017**, *118*, 083001.
- (16) Despré, V.; Golubev, N. V.; Kuleff, A. I. Charge Migration in Propiolic Acid: A Full Quantum Dynamical Study. *Phys. Rev. Lett.* **2018**, *121*, 203002.
- (17) Ayuso, D.; Palacios, A.; Decleva, P.; Martín, F. Ultrafast charge dynamics in glycine induced by attosecond pulses. *Phys. Chem. Chem. Phys.* **2017**, *19*, 19767–19776.
- (18) Bruner, A.; Hernandez, S.; Mauger, F.; Abanador, P. M.; LaMaster, D. J.; Gaarde, M. B.; Schafer, K. J.; Lopata, K. Attosecond Charge Migration with TDDFT: Accurate Dynamics from a Well-Defined Initial State. *J. Phys. Chem. Lett.* **2017**, *8*, 3991.
- (19) Jia, D.; Manz, J.; Paulus, B.; Pohl, V.; Tremblay, J. C.; Yang, Y. Quantum control of

- electronic fluxes during adiabatic attosecond charge migration in degenerate superposition states of benzene. *Chem. Phys.* **2017**, *482*, 146–159.
- (20) Perfetto, E.; Sangalli, D.; Marini, A.; Stefanucci, G. Ultrafast Charge Migration in XUV Photoexcited Phenylalanine: A First-Principles Study Based on Real-Time Nonequilibrium Green’s Functions. *J. Phys. Chem. Lett.* **2018**, *9*, 1353–1358.
- (21) Folorunso, A. S.; Bruner, A.; Mauger, F. m. c.; Hamer, K. A.; Hernandez, S.; Jones, R. R.; DiMauro, L. F.; Gaarde, M. B.; Schafer, K. J.; Lopata, K. Molecular Modes of Attosecond Charge Migration. *Phys. Rev. Lett.* **2021**, *126*, 133002.
- (22) Lopata, K.; Govind, N. Modeling Fast Electron Dynamics with Real-Time Time-Dependent Density Functional Theory: Application to Small Molecules and Chromophores. *J. Chem. Theory Comput.* **2011**, *7*, 1344–1355.
- (23) Aprà, E. et al. NWChem: Past, present, and future. *J. Chem. Phys.* **2020**, *152*, 184102.
- (24) Acebrón, J. A.; Bonilla, L. L.; Pérez Vicente, C. J.; Ritort, F.; Spigler, R. The Kuramoto model: A simple paradigm for synchronization phenomena. *Rev. Mod. Phys.* **2005**, *77*, 137–185.
- (25) Feldhaus, J.; Arthur, J.; Hastings, J. X-ray free-electron lasers. *J. Phys. B: At. Mol. Opt. Phys.* **2005**, *38*, S799–S819.
- (26) Pikovsky, A.; Rosenblum, M. Synchronization. *Scholarpedia* **2007**, *2*, 1459.
- (27) Hoerner, P.; Schlegel, H. B. Angular Dependence of Strong Field Ionization of Haloacetylenes HCCX (X = F, Cl, Br, I), Using Time-Dependent Configuration Interaction with an Absorbing Potential. *J. Phys. Chem. C* **2018**, *122*, 13751.
- (28) Sándor, P.; Sissay, A.; Mauger, F.; Gordon, M. W.; Gorman, T. T.; Scarborough, T. D.; Gaarde, M. B.; Lopata, K.; Schafer, K. J.; Jones, R. R. Angle-dependent strong-field ionization of halomethanes. *J. Chem. Phys.* **2019**, *151*, 194308.

- (29) Kohn, W.; Sham, L. J. Self-Consistent Equations Including Exchange and Correlation Effects. *Phys. Rev.* **1965**, *140*, A1133–A1138.
- (30) Eshuis, H.; van Voorhis, T. The influence of initial conditions on charge transfer dynamics. *Phys. Chem. Chem. Phys.* **2009**, *11*, 10293–10298.
- (31) Helbig, N.; Fuks, J. I.; Casula, M.; Verstraete, M. J.; Marques, M. A. L.; Tokatly, I. V.; Rubio, A. Density functional theory beyond the linear regime: Validating an adiabatic local density approximation. *Phys. Rev. A* **2011**, *83*, 032503.
- (32) Legrand, C.; Suraud, E.; Reinhard, P.-G. Comparison of self-interaction-corrections for metal clusters. *J. Phys. B: At. Mol. Opt. Phys.* **2002**, *35*, 1115.
- (33) Javanainen, J.; Eberly, J. H.; Su, Q. Numerical simulations of multiphoton ionization and above-threshold electron spectra. *Phys. Rev. A* **1988**, *38*, 3430–3446.
- (34) Laskar, J. Frequency analysis for multi-dimensional systems. Global dynamics and diffusion. *Physica D* **1993**, *67*, 257–281.
- (35) Laskar, J. In *Hamiltonian Systems with Three or More Degrees of Freedom*; Simó, C., Ed.; Springer Netherlands, 1999; p 134.